DOI: 10.1002/ejic.201100031

Reactions of Dimeric Aluminium Hydride Compounds Containing Bidentate Dianionic Pyrrolyl Ligands and Their Applications in Ring-Opening Polymerization of ε-Caprolactone

Ya-Chi Chen,[a] Che-Yu Lin,[a] Wen-Yen Huang,[a] Amitabha Datta,[a] Jui-Hsien Huang,*[a] Meng-Shiue Tsai,[b] Ting-Yu Lee,*[b] Cheng-Yi Tu,[a] and Ching-Han Hu[a]

Keywords: Aluminium / Hydrides / N ligands / Ring-opening polymerization

A series of dimeric aluminium compounds containing substituted bidentate dianionic pyrrolyl ligands have been synthesized and their reactivity and application in the ring-opening polymerization of ε-caprolactone have been studied. The reactions of $[\{C_4H_3N(2\text{-}CH_2N\textit{t}Bu)\}AlH]_2$ (**1**) with 2 equiv. of 1-indanone and 9-fluorenone in dichloromethane generated $[\{C_4H_3N(2\text{-}CH_2N\textit{t}Bu)\}Al(\mu\text{-}OC_9H_9)]_2$ (**2**) and $[\{C_4H_3N(2\text{-}CH_2N\textit{t}Bu)\}Al\{\mu\text{-}OCH(C_{12}H_8)\}]_2$ (**3**), respectively, by hydroalumination. Similarly, the reactions of **1** with 2 equiv. of 2-cyclohexen-1-one, 1-(2,4,6-trimethylphenyl)-1-ethanone, benzophenone, and 1,1-diphenylacetone in dichloromethane afforded N*t*Bu-bridged dialuminium compounds **4**–**7**, $[\{C_4H_3N(2\text{-}CH_2N\textit{t}Bu)\}Al(OR)]_2$ [**4**, R = C_6H_9; **5**, R = CH(Me)-(C_6H_2-2,4,6-Me_3); **6**, R = $CHPh_2$; **7**, R = CH(Me)-($CHPh_2$)] by insertion. A similar insertion occurred when **1** was treated with 2 equiv. of 2,4-pentandione and dibenzoylmethane in dichloromethane to yield N*t*Bu-bridged dioxylate aluminium dimeric compounds **8** and **9**, respectively. The Al atoms in compounds **2** and **4**–**7** possess a distorted tetrahedral geometry whereas the Al atoms in **8** and **9** have a square-pyramidal environment. All the compounds have been well characterized by NMR spectroscopy and compounds **2** and **4**–**9** in the solid state were subjected to X-ray diffraction analysis. A study of the polymerization of ε-caprolactone revealed that the activity of the Al complexes is largely reliant on the steric nature of the substituents of their alkoxide groups.

Introduction

Metal hydrides and their complexes are considered valuable synthons in chemistry. It has been demonstrated that main-group and transition-metal hydrides are important intermediates in some industrial processes and also function as catalysts.[1] Early-transition-metal hydride derivatives are thought to be responsible for an over abundance of organic transformations, catalytic cycles, and olefin polymerization intermediates or deactivation products.[2] The problems associated with the application of metal hydride complexes are the selectivity of the reduction and the solubility of the reducing agents even though some soluble hydride reagents such as $\textit{i}Bu_2AlH$, DIBALH, $LiAl(O\textit{t}Bu)_3H$, or superhydride $LiBEt_3H$ are commercially available. To overcome these problems, researchers have tried to introduce large organic ligands at the metal hydride centers to increase their steric controllability and solubility in organic solvents. From the point of view of ligand design, nitrogen donor ligands, for which in principle a great variety of synthetic strategies are available, may generate catalytically active complexes. Nitrogen-based polydentate ligands such as phenoxyimine[3–6] and 2,6-bis(*N*-aryliminomethyl)pyridine,[7] which serve as supporting ligands for polymerization catalysts, have attracted particular interest because of their advantageous ease of synthesizing and flexibility in introducing sterically and electronically demanding features into the ligand.[8,9] Concerning different ligand systems, the pyrrolyl entity has the ability to bring metal centers into close proximity and provides an intra- or intermolecular pathway for bonding interactions. Further changes in the substituents on the pyrrolyl ring can facilitate favorable configurations and control the metal polyhedron coordination. Aluminium hydride complexes with pyrrolyl-based ligands react with ketones to generate aluminium alkoxide complexes by hydroalumination[10] and we have also described the reactivity of monomeric aluminium hydride complexes with pyrrolyl ligands[11] in insertion and C–C coupling reactions. Thus, we have focused our research on finding new organoaluminium hydrides with ketiminate or donor-substituted pyrrole ligands and have discussed their

---

[a] Department of Chemistry, National Changhua University of Education,
50058 Changhua, Taiwan
E-mail: juihuang@cc.ncue.edu.tw
[b] Department of Applied Chemistry, National University of Kaohsiung,
811 Kaohsiung, Taiwan

Supporting information for this article is available on the WWW under http://dx.doi.org/10.1002/ejic.201100031.

reactions with PhNCO, CO_2, H_2O, and tertiary alcohols.[12] To extend our research of the above-mentioned aluminium hydride chemistry mediated by pyrrolyl-linked architectures, we report herein a series of novel aluminium complexes in different reaction conditions and their applications in the ring-opening polymerization of ε-caprolactone. All the products were investigated in detail by multinuclear NMR spectroscopy and seven compounds have also been characterized by single-crystal X-ray diffraction.

Results and Discussion

Reactions and Characterizations

The dimeric aluminium hydride compound **1** shows good reactivity towards unsaturated organofunctional groups such as C=O or C=NOH forming aluminium alkoxides or oximates.[13] The reactions of **1** with mono- and diketones are summarized in Scheme 1 and Scheme 2, respectively. The reactions of **1** with 2 equiv. of 1-indanone and 9-fluorenone in dichloromethane resulted in moderate yields of $[\{C_4H_3N(2\text{-}CH_2NtBu)\}Al(\mu\text{-}OC_9H_9)]_2$ (**2**) and $[\{C_4H_3N(2\text{-}CH_2NtBu)\}Al\{\mu\text{-}OCH(C_{12}H_8)\}]_2$ (**3**), respectively, by hydroalumination. Compounds **2** and **3** form dialkoxy-bridged dialuminium compounds by insertion of 1-indanone and 9-fluorenone into the aluminium hydride bonds. The methylene protons of CH_2NtBu show characteristic ^1H NMR resonances with two doublets at δ = 4.19 and 4.96 ppm for **2** and two doublets at δ = 3.94 and 4.74 ppm for **3**. The chemical shift of the methine proton of the bridged alkoxy fragment appears at δ = 5.55 and 5.89 ppm, respectively. The molecular geometries of **2** and **3** were also verified by ^1H–^{13}C HSQC 2D NMR spectroscopy. Again, the reactions of **1** with 2 equiv. of 2-cyclohexen-1-one, 1-(2,4,6-trimethylphenyl)-1-ethanone, benzophenone, and 1,1-diphenylacetone in dichloromethane afforded NtBu-bridged dialuminium compounds **4**–**7**, $[\{C_4H_3N(2\text{-}CH_2NtBu)\}Al(OR)]_2$ [**4**, R = C_6H_9; **5**, R = $CH(Me)(C_6H_2\text{-}2,4,6\text{-}Me_3)$; **6**, R = $CHPh_2$; **7**, R = $CH(Me)(CHPh_2)$]. The carbonyl group on insertion into Al–H readily generates terminal aluminium alkoxide dimeric compounds. All the chemical shifts of the methylene protons of CH_2NtBu in compounds **4**–**7** show two doublets at δ = 3.66–5.03 ppm. The molecular geometries of **4** and **5** were also verified by ^1H–^{13}C HSQC 2D NMR spectroscopy.

Thus, the alkoxide fragments can participate in bridging between the aluminium atoms (compounds **2** and **3**) or form terminal groups (compounds **4**–**7**), as discussed in the literature.[14] However, there is no trend to allow prediction of the bonding modes of the hydroalumination reaction. The geometries of these compounds should be determined entirely by electronic and steric effects.

The reaction of 2 equiv. of 2,4-pentandione with **1** in dichloromethane generated yellow NtBu-bridged diketiminate aluminium dimeric compound $[\{C_4H_3N(2\text{-}CH_2NtBu)\}Al\{\kappa O,\kappa O\text{-}(OCMeCHCOMe)\}]_2$ (**8**) in 71% yield (Scheme 2). The ^1H NMR spectrum of **8** at room temperature shows one broad signal at δ = 1.14 ppm for the methyl protons of the tBu group of the substituted pyrrolyl and the diketiminate fragments, which indicates a fast exchange of the geometry of this compound. The ^1H NMR spectrum of **8** in [D8]toluene at 0 °C reveals that the tBu groups and the methyl groups of the diketiminate fragments show several sharp singlets between 1.06–1.69 ppm, which indicates a slow exchange limit of the geometry at low tem-

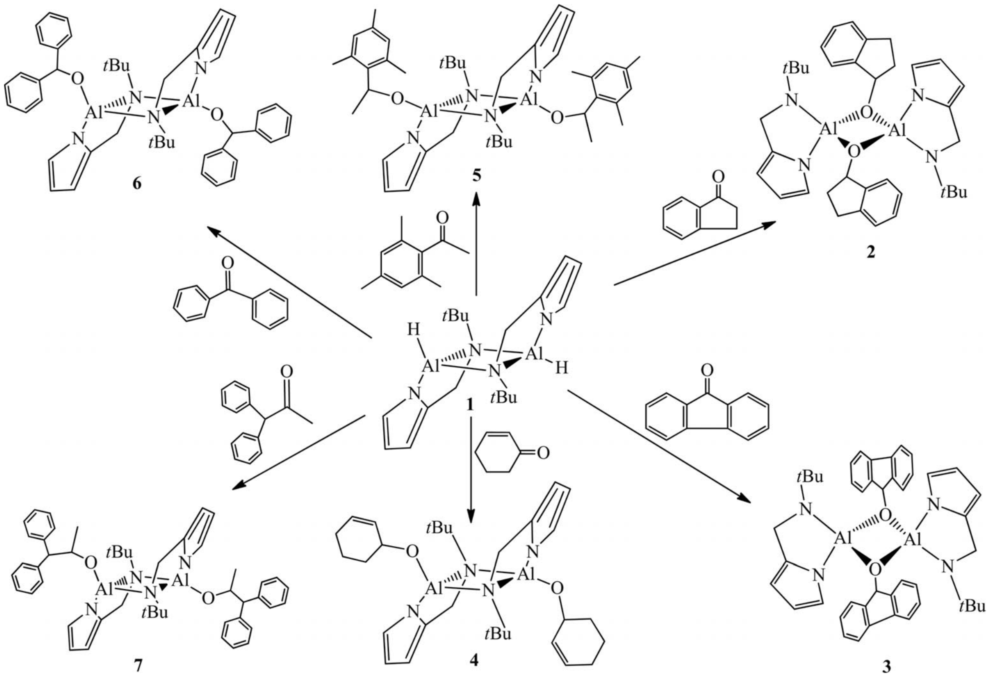

Scheme 1.

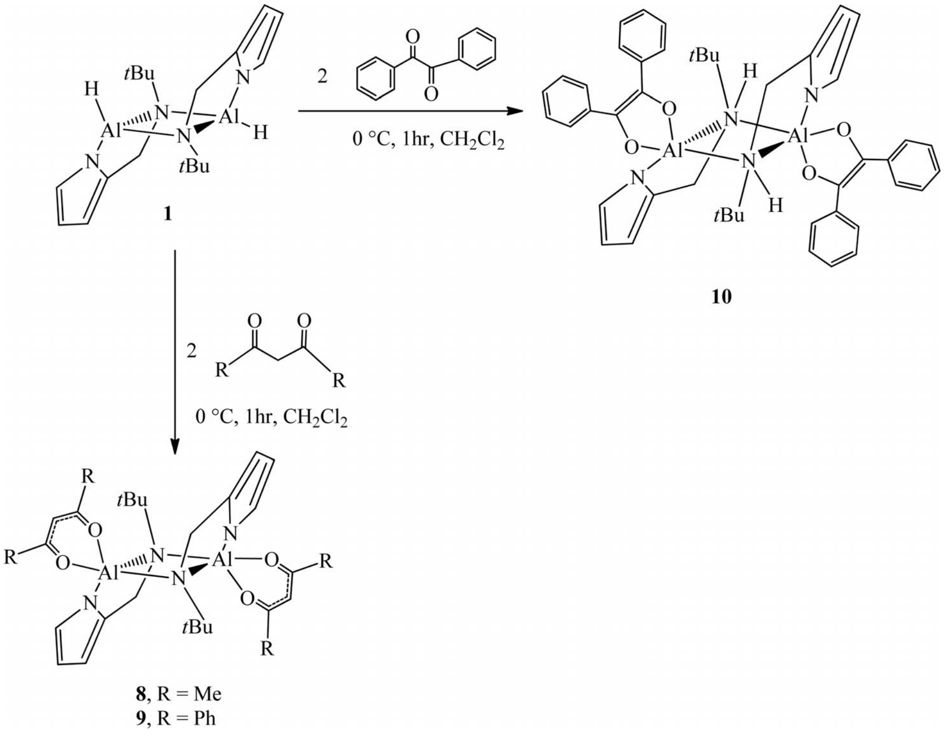

Scheme 2.

perature. In addition, two sharp singlets appear at δ = 4.13 and 5.09 ppm in a ratio of 2:1 assigned to the methylene protons of the $CH_2N\textit{t}Bu$ fragments and the methine protons of diketiminate further confirmed the geometry of compound **8**.

Again, the reaction of **1** with 2 equiv. of dibenzoylmethane in dichloromethane afforded an orange powder of $[\{C_4H_3N(2\text{-}CH_2N\textit{t}Bu)\}Al\{\kappa O,\kappa O\text{-}(OCPhCHCOPh)\}]_2$ (**9**) in 69% yield by deprotonation of one of the two methylene protons of the diketiminate backbone of the diketone ligands. The ^1H and ^{13}C NMR spectra of the methyl groups of the N*t*Bu fragments both show broad bands at δ = 1.27 and 30.1 ppm, respectively. The methylene protons of $CH_2N\textit{t}Bu$ appear as one singlet at δ = 4.28 ppm and an AB spin system in which two doublets are observed at δ = 4.24 and 4.69 ppm. The methine protons of the two diketiminate backbones are observed at δ = 7.03 and 7.18 ppm, which was also confirmed by ^1H–^{13}C HSQC 2D NMR spectra. All the information indicates that the geometry of **9** in solution is relatively rigid and shows an asymmetrical conformation.

The reaction of **1** with organic diketone benzil in dichloromethane at 0 °C in a 2:1 ratio resulted in diketonate compound $[\{C_4H_3N(2\text{-}CH_2NH\textit{t}Bu)\}Al\{\kappa O,\kappa O\text{-}(PhOC{=}COPh)\}]_2$ (**10**) in 47% yield. One triplet signal is observed at δ = 2.32 ppm in the ^1H NMR spectrum and has been assigned to the amino proton of the NH*t*Bu fragment. This was confirmed by the ^1H–^{13}C HSQC 2D and homonuclear decoupled ^1H NMR spectra. Apparently, the original dianionic pyrrolyl ligand $[C_4H_3N(2\text{-}CH_2N\textit{t}Bu)]^{2-}$ in compound **1** has been reprotonated to form a mono-anionic pyrrolyl ligand $[C_4H_3N(2\text{-}CH_2NH\textit{t}Bu)]^-$ in compound **10**. The ^1H NMR spectrum of **10** shows the methylene protons of $CH_2NH\textit{t}Bu$ as two multiplets at δ = 3.45 and 3.78 ppm. Although the proton signal (δ = 2.32 ppm) of NH*t*Bu is decoupled, the resonances for the methylene protons of $CH_2NH\textit{t}Bu$ are present as two simple doublets. In addition, the reaction of $[\{C_4H_3N(2\text{-}CH_2N\textit{t}Bu)\}AlD]_2$ (**1-D**), obtained from the reaction of $AlD_3{\cdot}NMe_3$ and $[C_4H_3NH(2\text{-}CH_2NH\textit{t}Bu)]$, with benzil afforded $[\{C_4H_3N(2\text{-}CH_2ND\textit{t}Bu)\}Al\{\kappa O,\kappa O\text{-}(PhOC{=}COPh)\}]_2$ (**10-D**). No resonance is observed at δ = 2.32 ppm in the ^1H NMR spectrum, which indicates that the amino proton of NH*t*Bu has been replaced by the deuterium atom in **10-D**. A possible reaction mechanism is shown in Scheme 3. Compound **1-D** reacts with benzil by hydroalumination to form an aluminium ketone–alkoxide intermediate and then the amido nitrogen of the $CH_2N\textit{t}Bu$ extracts one proton from the ketone–alkoxide fragment to form an ene–diolate intermediate. The same procedure is repeated again to form the final product **10-D**. The reduction of benzil to diphenylethene–diolate using low-valent metal complexes has been reported in the literature,[15] however, there is no report of the reduction by metal complexes in high oxidation states. Metal hydride induced benzil reduction to diphenylethene–diolate is even less well explored.[11] Previously dialuminium compounds were generated with mono- or bidentate orientation of acetone or acetone oxime into $[\{C_4H_3N(2\text{-}CH_2N\textit{t}Bu)\}AlH]_2$,[13] whereas in this work we prepared two dialkoxy-bridged dialuminium compounds by insertion of 1-indanone and 9-fluorenone into the aluminium hydride bonds.

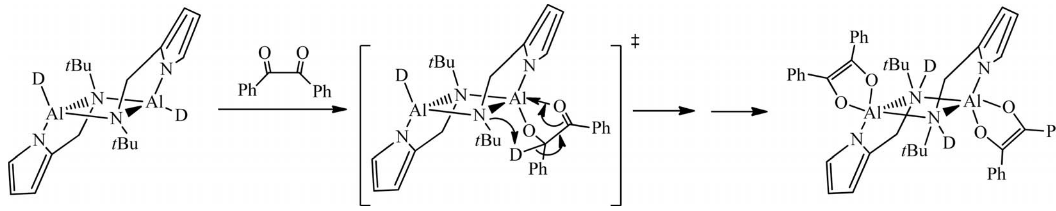

Scheme 3.

Molecular Structures of 2 and 4–9

Crystals of **2** and **4**–**9** suitable for X-ray analysis were obtained by the evaporation of different solvents. The details of data collection and selected bond lengths and angles are shown in Table 1 and Table 2, respectively. Crystals of **2** were generated from a mixture of toluene and pentane at –20 °C and possess a center of symmetry. The molecular geometry of **2**, shown in Figure 1, may be described as an Al_2O_2 parallelogram into which two O atoms from each indanone molecule bridge the two aluminium atoms with Al(1)–O(1)–Al(1A) and O(1)–Al(1)–O(1A) angles of 99.35(4) and 80.65(4)°, respectively. The substituted pyrrolyl ligands chelate an aluminium atom with a bite angle of 94.09(5)° and the corresponding Al(1)–N(1) and Al(1)–N(2) bond lengths are 1.8273(11) and 1.7791(10) Å, respectively. The Al–N(*t*Bu) bond length is shorter than that of Al–N(pyrrolyl), which indicates the stronger σ-donating ability of the N*t*Bu fragment to the Al atom. The two aluminium atoms adopt a distorted tetrahedral geometry consisting of a (NNOO) coordination mode generated by bidentate orientation of the pyrrolyl ligand and bridging of the indanone O atoms. The Al–N(pyrrolyl) bond lengths are rather similar to those of previously reported aluminium pyrrolyl compounds.[13]

The solid-state structures of compounds **4**–**7** were determined similarly and their molecular structures are shown in Figures 2, 3, 4 and 5, respectively. There are two independent molecules of **4** in one unit cell and the disordered cyclohexenyl fragment shows a carbon–carbon double bond length of 1.260(7) Å. Compounds **4**–**7** all possess a distorted tetrahedral geometry around the central aluminium center as a result of the coordination of the bidentate pyrrolyl ligand and two oxygen atoms from 2-cyclohexen-1-one, 1-(2,4,6-trimethylphenyl)-1-ethanone, benzophenone, and 1,1-diphenylacetone, respectively. The two aluminium atoms and two bridging nitrogen atoms of the N*t*Bu fragments form an Al_2N_2 parallelogram with Al–N–Al bond angles and Al–N bond lengths ranging from 90.89(10)–91.34(6)° and 1.9395(9)–1.9766(2) Å, respectively. The two pyrrolyl rings shuffle in the *trans* positions of the Al_2N_2 plane presumably due to steric congestion. The lengths of the bonds between the aluminium atoms and the terminal

Table 1. Crystal data for compounds **2** and **4**–**9**.

	2	4	5	6	7	8	9
Formula	$C_{21.5}H_{27}AlN_2O$	$C_{30}H_{46}Al_2N_4O_2$	$C_{40}H_{58}Al_2N_4O_2$	$C_{44}H_{50}Al_2N_4O_2$	$C_{62}H_{74}Al_2N_4O_2$	$C_{28}H_{42}Al_2N_4O_4$	$C_{50}H_{54}Al_2Cl_4N_4O_4$
M_r	356.43	548.67	680.86	720.84	961.21	552.62	970.73
Crystal system	triclinic	triclinic	triclinic	triclinic	triclinic	monoclinic	monoclinic
Space group	$P\bar{1}$	$P\bar{1}$	$P\bar{1}$	$P\bar{1}$	$P\bar{1}$	$P2_1/n$	$C2/c$
a [Å]	9.3554(4)	9.8142(3)	8.705(3)	9.8094(7)	9.5164(2)	14.8664(7)	28.1450(14)
b [Å]	10.2952(4)	10.0249(4)	8.709(3)	10.2384(7)	10.1659(3)	12.1660(6)	12.2188(6)
c [Å]	11.9025(5)	15.3380(5)	13.712(5)	10.7064(8)	14.8496(4)	17.7969(8)	17.1129(8)
α [°]	107.160(2)	90.074(2)	89.527(6)	72.5830(10)	100.790(2)		
β [°]	98.425(2)	93.162(2)	72.007(7)	74.8260(10)	95.017(2)	113.2050(10)	124.482(3)
γ [°]	109.793(2)	93.573(2)	79.420(6)	70.5330(10)	104.1840(10)		
V [Å^3], Z	991.18(7), 2	1503.81(9), 2	970.6(6), 1	951.51(12), 1	1354.70(6), 1	2958.4(2), 4	4851.1(4), 4
$D_{calcd.}$ [Mg m^{-3}]	1.194	1.212	1.165	1.258	1.178	1.241	1.329
Absol. coeff. [mm^{-1}]	0.114	0.130	0.113	0.120	0.100	0.137	0.329
T [K]	150(2)	150(2)	150(2)	150(2)	150(2)	150(2)	150(2)
F(000)	382	592	368	384	516	1184	2032
Reflections collected	15209	31599	14004	14292	26441	22902	18165
Independent refl.	4744	7768	4672	4592	5868	7146	5036
	(R_{int} = 0.0193)	(R_{int} = 0.0575)	(R_{int} = 0.0569)	(R_{int} = 0.0242)	(R_{int} = 0.0288)	(R_{int} = 0.0523)	(R_{int} = 0.0438)
Data/restraints/params	4744/0/254	7768/0/380	4672/0/224	4592/0/238	5868/0/321	7146/0/353	5036/2/351
Goodness of fit on F^2	1.070	0.981	1.036	1.046	1.075	1.042	1.007
Final R indices	$R1$ = 0.0383	$R1$ = 0.0774	$R1$ = 0.0401	$R1$ = 0.0351	$R1$ = 0.0497	$R1$ = 0.0536	$R1$ = 0.0660
[$I > 2\sigma(I)$]	$wR2$ = 0.1076	$wR2$ = 0.1950	$wR2$ = 0.1183	$wR2$ = 0.963	$wR2$ = 0.1351	$wR2$ = 0.1243	$wR2$ = 0.1839
R indices	$R1$ = 0.0468	$R1$ = 0.1277	$R1$ = 0.0803	$R1$ = 0.0392	$R1$ = 0.0686	$R1$ = 0.1017	$R1$ = 0.1057
(all data)	$wR2$ = 0.1128	$wR2$ = 0.2241	$wR2$ = 0.1372	$wR2$ = 0.992	$wR2$ = 0.1459	$wR2$ = 0.1427	$wR2$ = 0.2230
Largest diff. peak/hole [e Å^{-3}]	0.375/–0.225	0.734/–0.571	0.474/–0.584	0.304/–0.305	0.797/–0.287	0.601/–0.325	0.773/–0.653

Table 2. Selected bond lengths [Å] and angles [°] for compounds **2** and **4**–**9**.

	2		
Al(1)–N(2)	1.7791(10)	Al(1)–O(1)	1.8175(9)
Al(1)–O(1A)	1.8229(9)	Al(1)–N(1)	1.8273(11)
O(1)–C(10)	1.4756(15)		
N(2)–Al(1)–O(1)	122.59(5)	N(2)–Al(1)–O(1A)	127.21(5)
O(1)–Al(1)–O(1A)	80.65(4)	N(2)–Al(1)–N(1)	94.09(5)
O(1)–Al(1)–N(1)	120.60(5)	C(10)–O(1)–Al(1)	129.27(7)
C(10)–O(1)–Al(1A)	129.20(7)	Al(1)–O(1)–Al(1A)	99.35(4)
	4		
Al(1)–O(1)	1.674(3)	Al(1)–N(1)	1.825(3)
Al(1)–N(2A)	1.940(3)	Al(1)–N(2)	1.957(2)
N(2)–Al(1A)	1.940(3)	C(10)–C(11)	1.526(8)
C(11)–C(12)	1.260(7)	C(12)–C(13)	1.528(7)
C(13)–C(14)	1.501(8)	C(14)–C(15)	1.442(8)
O(1)–Al(1)–N(1)	116.75(14)	O(1)–Al(1)–N(2A)	112.08(13)
N(1)–Al(1)–N(2A)	118.66(12)	O(1)–Al(1)–N(2)	124.91(12)
N(1)–Al(1)–N(2)	91.74(12)	N(1)–Al(1)–N(2)	89.11(10)
Al(1A)–N(2)–Al(1)	90.89(10)	C(10)–O(1)–Al(1)	121.4(3)
	5		
Al(1)–O(1)	1.7049(12)	Al(1)–N(1)	1.8320(15)
Al(1)–N(2)	1.9766(12)	Al(1)–N(2A)	1.9358(13)
C(11)–O(1)	1.4364(17)	N(2)–Al(1A)	1.9358(13)
C(10)–C(11)	1.521(2)	C(11)–C(12)	1.532(2)
O(1)–Al(1)–N(1)	114.70(6)	O(1)–Al(1)–N(2)	127.94(6)
N(1)–Al(1)–N(2)	91.62(6)	O(1)–Al(1)–N(2A)	109.86(6)
Al(1A)–N(2)–Al(1)	91.34(6)	N(1)–Al(1)–N(2A)	122.14(6)
N(2A)–Al(1)–N(2)	88.66(6)	C(11)–O(1)–Al(1)	127.66(11)
	6		
Al(1)–O(1)	1.7129(8)	Al(1)–N(1)	1.8305(9)
Al(1)–N(2)	1.9395(9)	Al(1)–N(2A)	1.9656(9)
C(10)–O(1)	1.4241(12)	N(2)–Al(1A)	1.9656(9)
O(1)–Al(1)–N(1)	115.84(4)	O(1)–Al(1)–N(2)	113.10(4)
N(1)–Al(1)–N(2)	119.03(4)	O(1)–Al(1)–N(2A)	123.99(4)
Al(1)–N(2)–Al(1A)	91.03(4)	N(1)–Al(1)–N(2A)	92.22(4)
N(2)–Al(1)–N(2A)	88.97(4)	C(10)–O(1)–Al(1)	126.48(7)
	7		
Al(1)–O(1)	1.6712(14)	Al(1)–N(1)	1.8316(15)
Al(1)–N(2)	1.9644(15)	Al(1)–N(2A)	1.9471(15)
C(11)–O(1)	1.407(2)	N(2)–Al(1A)	1.9471(15)
C(10)–C(11)	1.509(3)	C(11)–C(12)	1.536(3)
O(1)–Al(1)–N(1)	117.07(7)	O(1)–Al(1)–N(2)	125.69(7)
N(1)–Al(1)–N(2)	92.01(6)	O(1)–Al(1)–N(2A)	111.03(7)
Al(1A)–N(2)–Al(1)	91.09(6)	N(1)–Al(1)–N(2A)	118.79(7)
N(2A)–Al(1)–N(2)	88.91(6)	C(11)–O(1)–Al(1)	149.75(12)
	8		
Al(1)–O(2)	1.8106(17)	Al(1)–N(3)	1.871(2)
Al(1)–O(1)	1.8963(16)	Al(1)–N(2)	1.9586(19)
Al(1)–N(4)	2.1055(19)	Al(2)–N(4)	1.936(2)
Al(2)–N(2)	2.152(2)		
O(2)–Al(1)–N(3)	125.57(8)	O(2)–Al(1)–O(1)	89.55(7)
N(3)–Al(1)–O(1)	89.05(8)	O(2)–Al(1)–N(2)	108.17(8)
N(3)–Al(1)–N(2)	125.82(8)	O(1)–Al(1)–N(2)	98.42(8)
O(2)–Al(1)–N(4)	93.29(8)	N(3)–Al(1)–N(4)	84.72(8)
O(1)–Al(1)–N(4)	173.70(8)	N(2)–Al(1)–N(4)	86.05(8)
O(4)–Al(2)–N(2)	177.22(8)	Al(1)–N(2)–Al(2)	92.33(8)
	9		
Al(1)–O(1)	1.816(2)	Al(1)–N(1)	1.871(3)
Al(1)–O(2)	1.909(2)	Al(1)–N(2)	1.939(3)
Al(1)–N(2A)	2.139(3)	C(16)–O(2)	1.278(4)
C(18)–O(1)	1.312(4)	C(11)–C(12)	1.361(6)
O(1)–Al(1)–N(1)	116.69(112)	O(1)–Al(1)–O(2)	89.50(10)
N(1)–Al(1)–O(2)	87.47(11)	O(1)–Al(1)–N(2)	121.25(11)
Al(1)–N(2)–Al(1A)	95.05(10)	N(1)–Al(1)–N(2)	122.05(11)
N(1)–Al(1)–N(2A)	84.52(10)	O(2)–Al(1)–N(2A)	169.08(10)
O(2)–Al(1)–N(2)	93.17(10)	N(2)–Al(1)–N(2A)	84.52(10)

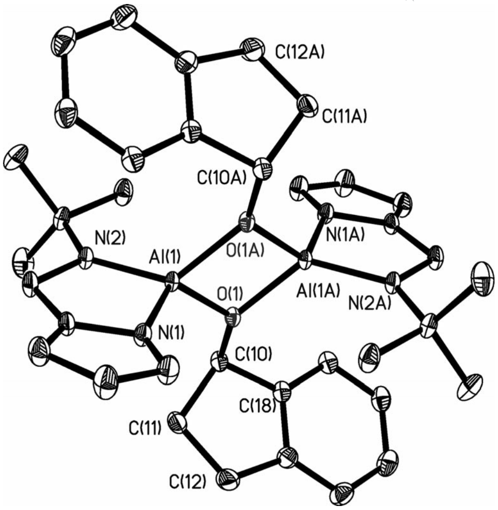

Figure 1. Molecular structure of compound **2**. Thermal ellipsoids are drawn at the 30% probability level. The toluene molecules and hydrogen atoms have been omitted for clarity.

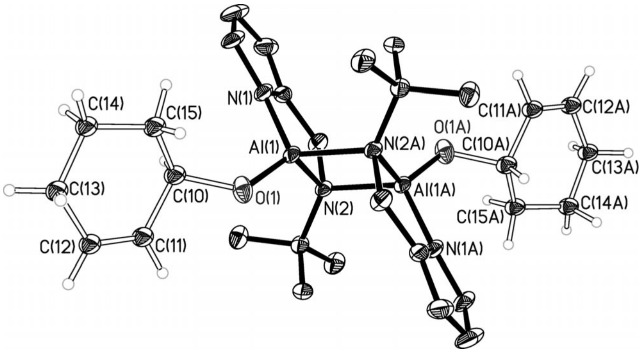

Figure 2. Molecular structure of compound **4**. Thermal ellipsoids are drawn at the 30% probability level. The hydrogen atoms except those on the cyclohexyl ring have been omitted for clarity.

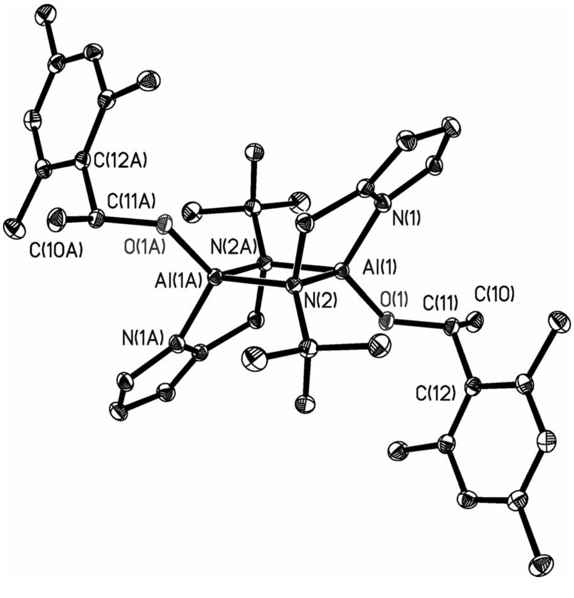

Figure 3. Molecular structure of compound **5**. Thermal ellipsoids are drawn at the 30% probability level. The hydrogen atoms have been omitted for clarity.

alkoxide oxygen atoms of compounds **4**–**7** are very similar and lie in the range 1.674(3)–1.7129(8) Å. However, the Al–O–C bond angle in **7** [149.75(12)°] is much larger than those in compounds **4**–**6** [121.4(3)–127.66(11)°], presumably due to the large steric congestion of the 1,1-diphenyl-2-propyl fragment.

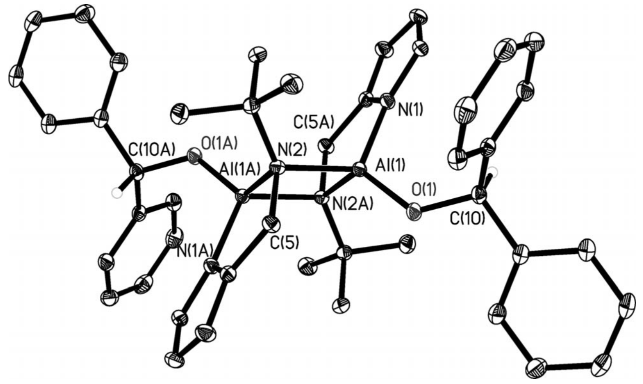

Figure 4. Molecular structure of compound **6**. Thermal ellipsoids are drawn at the 30 % probability level. The hydrogen atoms have been omitted for clarity.

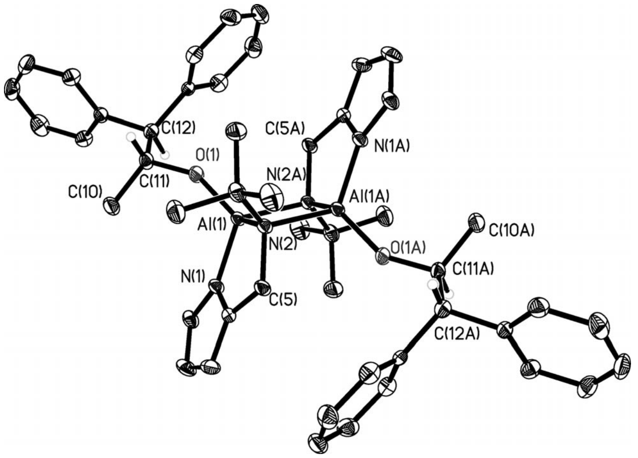

Figure 5. Molecular structure of compound **7**. Thermal ellipsoids are drawn at the 30 % probability level. The toluene molecules and the hydrogen atoms except the methane proton of the diphenylmethoxy group have been omitted for clarity.

The molecular structures of compounds **8** and **9** are shown in Figure 6 and Figure 7, respectively. For compound **8**, the two nitrogen atoms of the N*t*Bu fragments bridge two aluminum atoms forming an Al_2N_2 four-membered square with a dihedral angle of 14.2°. Again, the two pyrrolyl rings are located *trans* in the Al_2N_2 plane. Both the aluminium centers of **8** possess a five-coordinate geometry best described as distorted trigonal bipyramidal. One oxygen atom from the diketiminate fragment and one nitrogen atom from the bridged N*t*Bu fragment occupy the axial positions with O(1)–Al(1)–N(4) and O(4)–Al(2)–N(2) angles of 173.70(8) and 177.22(8)°, respectively.

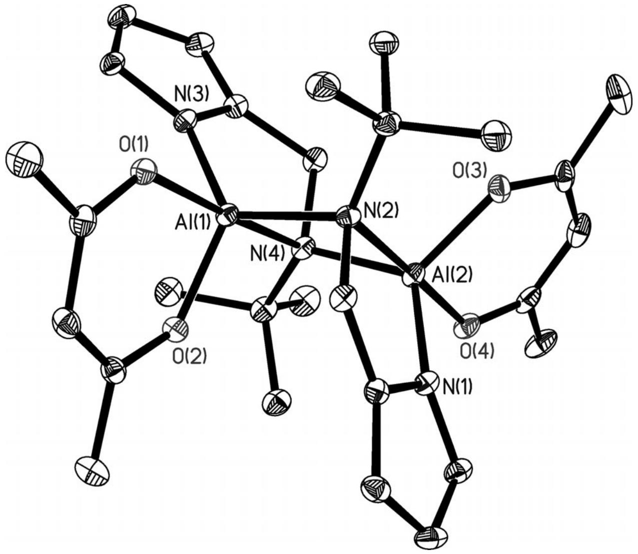

Figure 6. Molecular structure of compound **8**. Thermal ellipsoids are drawn at the 30 % probability level. The hydrogen atoms have been omitted for clarity.

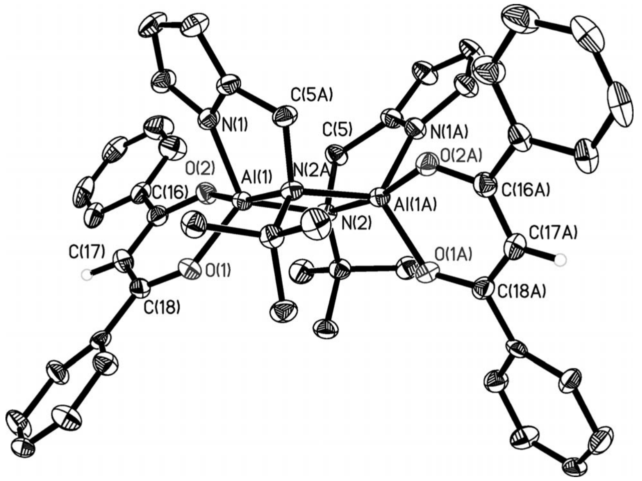

Figure 7. Molecular structure of compound **9**. Thermal ellipsoids are drawn at the 30 % probability level. The methylene molecules and hydrogen atoms have been omitted for clarity.

Unlike the geometry of **8**, compound **9** exhibits a center of symmetry in which the Al_2N_2 forms a perfect plane. Compound **9** consists of two five-coordinate aluminium centers, which can be described as distorted trigonal bipyramidal. One oxygen atom of the diketiminate ligand and one of the bridged N*t*Bu nitrogen atoms are located in axial positions with O(2)–Al(1)–N(2A) angles of 169.08(10)°. Note that the two pyrrolyl rings of **9** remain on the same side of the Al_2N_2 plane, presumably due to the large steric hindrance of the diphenyl–diketiminate ligands. Considering the Al_2N_2 parallelograms of the dimeric aluminium compounds containing bidentate ligands, similar geometries, presumably due to steric congestion, have been reported by several groups.[16] The Al–N bond lengths of the four-membered molecular units of compounds **4**–**7** [1.9395(9)–2.139(3) Å] are comparable to those previously published [1.993(2)–1.982(2) Å].[16] The Al–N–Al and N–Al–N bond angles of the molecular parallelograms of compounds **4**–**9** lie in the range 90.89(10)–95.05(10) and 86.05(8)–88.97(4)°, respectively, which are comparable to those of previously reported dimeric aminoalanes, 89.21(13) and 91.03(10)°,[16a] 88.8(1) and 91.2(1)°,[16b] 91.63(12) and 88.37(12)°,[16c] and 92.27(7) and 86.83(8)°.[16d]

Theoretical Calculations

The hydroalumination reactions of **1** with monoketones generated two different Al–alkoxide bonding modes, that is, bridged (compounds **2** and **3**) and terminal alkoxides (compounds **4**–**7**). The reasons for the bonding of the alkoxide fragment to aluminium at either terminal or bridging positions are still unclear. Therefore theoretical computations were performed by using the three-parameter hybrid of exact exchange and Becke's exchange energy functional,[17] plus Lee, Yang, and Parr's gradient-corrected correlation energy functional[18] (B3LYP). The Gaussian 03 suite of programs[19] was used in our study. The theoretical calculations show that the total formation energies of these compounds are determined by steric effects. The relative energies and dipole moments of the bridged (B) and terminal (T) forms of compounds **2**–**7**, determined by the DFT approach, are shown in Scheme 4. The calculations show that the bridged forms of compounds **2**–**7** have lower energies, but these results are only consistent with the experimental findings for compounds **2** and **3**. Note, the calculations can only be used to determine the gas-phase energies of compounds 2–7, which favor the bridged form. The possible reasons for the differences between the calculations and the results observed are solvent effects and different dipole moments of the molecules. Different solvents can affect the molecular geometry and crystal packing during product formation. In product formation, the solvent system and molecular dipole moment are crucial for determining the final geometries. The results shown in Scheme 4 demonstrate that the crystal packing (formation of the crystal) favors the terminal form due to larger dipole moments.

Ring-Opening Polymerization of ε-Caprolactone

Compounds **2**–**10** were used as catalysts in the ring-opening polymerization of ε-caprolactone.[20] The results are presented in Table 3. The aluminium alkoxides **2**–**7** showed good activity (entries 1–7) in the ring-opening polymerization of ε-caprolactone, giving very high conversions. The activity decreased in the order **7** ≈ **3** = **6** ≈ **5** > **4** ≈ **2**. Compounds **2** and **4** required a higher temperature and longer time than other catalysts to reach full conversion, which

Bridged form	Terminal form	E^a
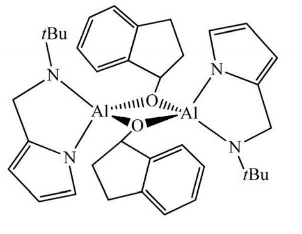 2B(0.003)	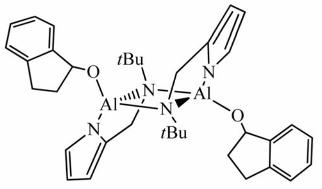 2T(0.783)	8.1
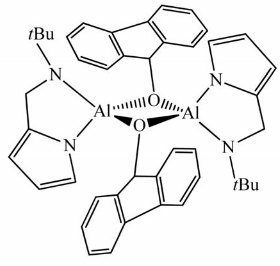 3B(0.008)	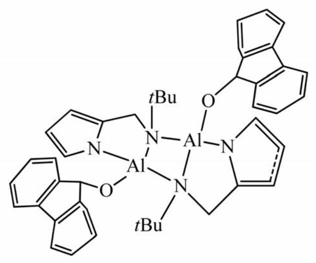 3T(1.177)	5.1
4B(0.157)	4T(0.259)	8.6
5B(0.033)	5T(0.656)	2.7
6B(0.020)	6T(0.0090)	0.0
7B(0.011)	7T(1.246)	1.6

Scheme 4. Relative energies [kcal/mol] of the terminal and bridged forms of the aluminium complexes and their dipole moments [Debye].

suggests that alkoxide groups with greater angles between the α carbon atoms and the neighboring two carbon atoms possess greater activity. These angles are around 113.0, 112.2, 113.0, 109.6, and 103.3° for **7**, **6**, **5**, **4**, and **2**, respectively. This phenomenon might be a result of bulky substituents on the α carbon of the alkoxides. However, the polymerization activities of the Al complexes might also be affected by the lability of the alkoxides towards dissociation or transformation of the dimeric aluminium species and the number of sites of initiation. Compounds **3** and **6** yielded PCL with higher M_w, which implies that the initiation efficiency strongly depends on the nature of the alkoxide as well as on the structure of the catalyst. The diketonate compounds **8**–**10** exhibited very low or no activity (entries 9–11) in the polymerization due to inertia of the ligands arising from the chelation of the alkoxides and therefore lack of initiation group. The range of the polydispersity index (PDI) of the poly(ε-caprolactone) product (1.26–1.47) is comparable to or a little broader than that of polymers obtained with other aluminium catalysts.[13,21]

Table 3. Polymerization of ε-caprolactone (CPL) using compounds **1**–**10** as catalysts.

	I[a]	Temp. [°C]/ time [min]	Conv. [%]	Activity [$g_{pol}\,mol_{cat}^{-1}\,h^{-1}$]	$M_{n,theor}$[b]	$M_{n,cor}$[c]	PDI
1	**2**	40/120	99	6000	11300	14494	1.47
2	**3**	40/30	100	24400	11414	17555	1.46
3	**4**	40/120	100	6050	11414	14027	1.43
4	**4**	25/120	77	4720	8789	7895	1.26
5	**5**	25/30	99	24200	11300	7001	1.26
6	**6**	25/30	100	24400	11414	31972	1.45
7	**7**	25/30	100	24600	11414	12111	1.37
8	**8**	40/1080	8	80	913	12285	1.42
9	**9**	40/1440	0	0	–	–	–
10	**10**	40/1440	0	0	–	–	–

[a] I = initiator. [b] $M_{n,theor} = ([CPL]_0/[\mathbf{4}]_0) \times 114.14 \times$ conversion [%] for CPL. [c] $M_{n,cor} = 0.259(M_{n,GPC,St})^{1.073}$ for CPL.[20]

Conclusions

The reactivities of $[\{C_4H_3N(2\text{-}CH_2N\textit{t}Bu)\}AlH]_2$ (**1**) with different ketones have been investigated and different types of products, formed by either hydroalumination or insertion reactions, were identified by NMR spectroscopic analyses. We chose $[\{C_4H_3N(2\text{-}CH_2N\textit{t}Bu)\}AlH]_2$ as a starting material because of its strong reactivity towards C=O-containing functional organic molecules. The aluminium dihydride shows high reactivity in these reactions. More interestingly, we prepared two new dialkoxy-bridged dialuminium complexes showing the reactivity of carbonyl towards hydroalumination. The activities of the Al complexes in the polymerization of ε-caprolactone are strongly dependent on the nature of the alkoxide groups. Future work will explore the mechanisms of the reactions of highly reactive symmetric aluminium dihydride compound **1** in several applications in organic synthesis.

Experimental Section

General Procedure: All reactions were performed under dry nitrogen using standard Schlenk or glove-box techniques. Toluene, diethyl ether, and tetrahydrofuran were dried by heating at reflux over sodium benzophenone ketyl. CH_2Cl_2 was dried with P_2O_5. All solvents were distilled and stored in solvent reservoirs containing 4 Å molecular sieves and were purged with nitrogen. ^1H and ^{13}C NMR spectra were recorded with a Bruker Avance 300 spectrometer. Chemical shifts for ^1H and ^{13}C NMR spectra are given in ppm relative to residual protons and ^{13}C in $CDCl_3$ (δ = 7.24, 77.0 ppm) and C_6D_6 (δ = 7.15, 128.0 ppm). Elemental analyses were performed with a Heraeus CHN-OS Rapid Elemental Analyzer at the Instrument Center, National Chung Hsing University. $[\{C_4H_3N(2\text{-}CH_2N\textit{t}Bu)\}AlH]_2$ (**1**) was prepared according to a previously reported procedure.[13] All the chemicals (Aldrich, Acros) were used as received.

$[\{C_4H_3N(2\text{-}CH_2N\textit{t}Bu)\}Al(OC_9H_9)]_2$ (2): 1-Indanone (0.38 g, 2.8 mmol) in dichloromethane (20 mL) solution was added through a cannula to a solution of **1** (0.50 g, 1.4 mmol) in dichloromethane (20 mL) at –78 °C. The reaction was complete within 30 min at room temperature and the volatiles were removed under vacuum to generate a pale-orange solid that was recrystallized from a toluene/pentane mixed solution at –20 °C to yield 0.37 g of the final product (42.5% yield). ^1H NMR ($CDCl_3$): δ = 0.74 (s, 18 H, $NCMe_3$), 2.02, 2.59 (m, 4 H, CH_2), 2.81, 3.03 (m, 4 H, CH_2), 4.19, 4.96 (dd, $^2J_{HH}$ = 16.5 Hz, 4 H, CH_2NCMe_3), 5.55 (t, J_{HH} = 6.6 Hz, 2 H, OCH), 6.07 (s, 2 H, pyrrolyl CH), 6.45 (s, 2 H, pyrrolyl CH), 6.69 (s, 2 H, pyrrolyl CH), 7.27 (s, 8 H, phenyl CH) ppm. $^{13}C\{^1H\}$ NMR ($CDCl_3$): δ = 28.7 (q, J_{CH} = 128 Hz, $NCMe_3$), 29.6 (t, J_{CH} = 130 Hz, CH_2), 38.6 (t, J_{CH} = 130 Hz, CH_2), 44.0 (t, J_{CH} = 138 Hz, CH_2NCMe_3), 56.7 (s, $NCMe_3$),76.7 (d, J_{CH} = 137 Hz, OCH), 103.4 (d, J_{CH} = 166 Hz, pyrrolyl CH), 114.1 (d, J_{CH} = 167 Hz, pyrrolyl CH), 120.5 (d, J_{CH} = 181 Hz, pyrrolyl CH), 123.9 (d, J_{CH} = 157 Hz, phenyl CH), 124.7 (d, J_{CH} = 157 Hz, phenyl CH), 126.3 (d, J_{CH} = 160 Hz, phenyl CH), 127.4 (d, J_{CH} = 159 Hz, phenyl CH), 137.2 (s, pyrrolyl C_{ipso}), 142.4 (s, phenyl C_{ipso}), 147.2 (s, phenyl C_{ipso}) ppm.

$[\{C_4H_3N(2\text{-}CH_2N\textit{t}Bu)\}Al\{OCH(C_{12}H_8)\}]_2$ (3): Similar procedures as for compound **2** were used to synthesize **3**. Reactants **1** (0.50 g, 1.4 mmol) and 9-fluorenone (0.52 g, 2.8 mmol) were used and the reaction was carried out at room temperature for 1 h. A dark-purple solid was obtained in 63.2% yield (0.636 g). ^1H NMR ($CDCl_3$): δ = 0.89 (s, 18 H, $NCMe_3$), 3.94, 4.74 (dd, $^2J_{HH}$ = 16.8 Hz, 4 H, CH_2NCMe_3), 5.28 (s, 2 H, CH_2Cl_2), 5.89 (br. s, 4 H, OCH, pyrrolyl CH), 6.30 (t, J_{HH} = 2.7 Hz, 2 H, pyrrolyl CH), 6.33 (s, 2 H, pyrrolyl CH), 7.23–7.66 (m, 16 H, $C_{12}H_8$) ppm. $^{13}C\{^1H\}$ NMR ($CDCl_3$): δ = 28.6 (q, J_{CH} = 126 Hz, $NCMe_3$), 44.0 (t, J_{CH} = 141 Hz, CH_2NCMe_3), 56.8 (s, $NCMe_3$), 75.9 (d, J_{CH} = 144 Hz, OCH), 103.3 (d, J_{CH} = 165 Hz, pyrrolyl CH), 113.9 (d, J_{CH} = 172 Hz, pyrrolyl CH), 119.8 (d, J_{CH} = 154 Hz, phenyl CH), 120.8 (d, J_{CH} = 182 Hz, pyrrolyl CH), 125.3 (d, J_{CH} = 161 Hz, phenyl CH), 127.5 (d, J_{CH} = 164 Hz, phenyl CH), 128.5 (d, J_{CH} = 159 Hz, phenyl CH), 136.9 (s, pyrrolyl C_{ipso}), 139.7 (s, phenyl C_{ipso}), 147.2 (s, phenyl C_{ipso}) ppm.

$[\{C_4H_3N(2\text{-}CH_2N\textit{t}Bu)\}Al(OC_6H_9)]_2$ (4): Similar procedures as for compound **2** were used to synthesize **4**. Reactants **1** (0.50 g, 1.4 mmol) and 2-cyclohexen-1-one (0.280 mL, 2.8 mmol) were used and the reaction was carried out at room temperature for 1 h. An orange solid was obtained that was recrystallized from a dichloromethane/pentane mixed solution at –20 °C to yield 0.36 g of the final product (yield 46.8%). ^1H NMR ($CDCl_3$): δ = 0.74 (s, 18 H, $NCMe_3$), 1.56–2.01 (m, 12 H, cyclohexene CH_2), 4.13, 4.87 (dd,

$^2J_{HH}$ = 17.1 Hz, 4 H, C*H*$_2$NCMe$_3$), 4.47 (br., 2 H, OCH), 5.69, 5.73 (m, 4 H, cyclohexene CH), 5.98 (s, 2 H, pyrrolyl CH), 6.37 (t, J_{HH} = 2.4 Hz, 2 H, pyrrolyl CH), 6.74 (s, 2 H, pyrrolyl CH) ppm. ^{13}C{^{1}H} NMR (CDCl$_3$): δ = 19.7 (t, J_{CH} = 129 Hz, cyclohexene CH$_2$), 25.1 (t, J_{CH} = 124 Hz, cyclohexene CH$_2$), 28.6 (q, J_{CH} = 124 Hz, NC*Me*$_3$), 34.5 (t, J_{CH} = 130 Hz, cyclohexene CH$_2$), 43.9 (t, J_{CH} = 140 Hz, *C*H$_2$NCMe$_3$), 56.7 (s, N*C*Me$_3$), 66.5 (d, J_{CH} = 141 Hz, OCH), 103.0 (d, J_{CH} = 167 Hz, pyrrolyl CH), 113.8 (d, J_{CH} = 170 Hz, pyrrolyl CH), 120.4 (d, J_{CH} = 181 Hz, pyrrolyl CH), 128.1 (d, J_{CH} = 153 Hz, cyclohexene CH), 132.8 (d, J_{CH} = 157 Hz, cyclohexene CH), 137.5 (s, pyrrolyl C$_{ipso}$) ppm.

[{C$_4$H$_3$N(2-CH$_2$N*t*Bu)}Al{OCH(Me)(C$_6$H$_2$-2,4,6-Me$_3$)}]$_2$ (5): Similar procedures as for compound **2** were used to synthesize **5**. Reactants **1** (0.50 g, 1.4 mmol) and 1-(2,4,6-trimethylphenyl)-1-ethanone (0.46 g, 2.8 mmol) were used and the reaction was carried out at room temperature for 1 h. A pale-pink solid was obtained that was recrystallized from a dichloromethane/heptane mixed solution at –20 °C to yield 0.584 g of the final product (yield 61.2%). ^{1}H NMR (CDCl$_3$): δ = 0.87 (s, 18 H, NCMe$_3$), 1.56 (d, J_{HH} = 6.6 Hz, 3 H, OCH*CH*$_3$), 2.13 (br. s, 3 H, phenyl CH$_3$), 2.20 (s, 3 H, phenyl CH$_3$), 2.54 (br. s, 3 H, phenyl CH$_3$), 4.10, 4.81 (dd, $^2J_{HH}$ = 16.5 Hz, 4 H, C*H*$_2$NCMe$_3$), 5.60 (q, J_{HH} = 2.8 Hz, OC*H*CH$_3$), 5.98 (s, 2 H, pyrrolyl CH), 6.39 (t, J_{HH} = 2.4 Hz, 2 H, pyrrolyl CH), 6.73 (s, 4 H, pyrrolyl CH, phenyl CH) ppm. ^{13}C{^{1}H} NMR (CDCl$_3$): δ = 20.5 (q, J_{CH} = 139 Hz, phenyl CH$_3$), 20.6 (q, J_{CH} = 139 Hz, phenyl CH$_3$), 20.7 (q, J_{CH} = 129 Hz, phenyl CH$_3$), 24.9 (q, J_{CH} = 126 Hz, OCH*C*H$_3$), 28.3 (q, J_{CH} = 127 Hz, NC*Me*$_3$), 45.6 (t, J_{CH} = 140 Hz, *C*H$_2$NCMe$_3$), 56.5 (s, N*C*Me$_3$), 67.5 (q, J_{CH} = 139 Hz, O*C*HCH$_3$), 103.4 (d, J_{CH} = 168 Hz, pyrrolyl CH), 114.0 (d, J_{CH} = 164 Hz, pyrrolyl CH), 120.5 (m, pyrrolyl CH, phenyl CH), 135.5 (s, phenyl C$_{ipso}$), 137.1 (s, phenyl C$_{ipso}$), 139.0 (s, pyrrolyl C$_{ipso}$) ppm.

[{C$_4$H$_3$N(2-CH$_2$N*t*Bu)}Al{OCH(C$_6$H$_5$)$_2$}]$_2$ (6): Similar procedures as for compound **2** were used to synthesize **6**. Reactants **1** (0.50 g, 1.4 mmol) and benzophenone (0.52 g, 2.8 mmol) were used and the reaction was carried out at room temperature for 1 h. A yellow-brown solid was obtained that was recrystallized from a dichloromethane/diethyl ether mixed solution at –20 °C to yield 0.502 g of the final product (yield 49.7%). ^{1}H NMR (CDCl$_3$): δ = 0.89 (s, 18 H, NCMe$_3$), 4.24, 5.03 (dd, $^2J_{HH}$ = 16.7 Hz, 4 H, C*H*$_2$NCMe$_3$), 6.09 (s, 2 H, Ph$_2$C*H*O), 6.11 (s, 2 H, pyrrolyl CH), 6.25 (t, J_{HH} = 1.1 Hz, 2 H, pyrrolyl CH), 6.37 (s, 2 H, pyrrolyl CH), 7.15–7.49 (m, 20 H, phenyl CH) ppm. ^{13}C{^{1}H} NMR (CDCl$_3$): δ = 28.5 (q, J_{CH} = 125 Hz, NC*Me*$_3$), 43.8 (t, J_{CH} = 140 Hz, *C*H$_2$NCMe$_3$), 56.8 (s, N*C*Me$_3$), 77.1 (d, J_{CH} = 141 Hz, Ph$_2$*C*HO), 103.7 (d, J_{CH} = 167 Hz, pyrrolyl CH), 114.0 (d, J_{CH} = 169 Hz, pyrrolyl CH), 121.0 (d, J_{CH} = 182 Hz, pyrrolyl CH), 125.9 (d, J_{CH} = 161 Hz, phenyl CH), 126.2 (d, J_{CH} = 154 Hz, phenyl CH), 126.7 (d, J_{CH} = 160 Hz, phenyl CH), 127.1 (d, J_{CH} = 160 Hz, phenyl CH), 128.1 (d, J_{CH} = 160 Hz, phenyl CH), 128.3 (d, J_{CH} = 160 Hz, phenyl CH), 136.8 (s, pyrrolyl C$_{ipso}$), 146.1 (s, phenyl C$_{ipso}$), 147.0 (s, phenyl C$_{ipso}$) ppm.

[{C$_4$H$_3$N(2-CH$_2$N*t*Bu)}Al{OCH(Me)(CHPh$_2$)}]$_2$ (7): Similar procedures as for compound **2** were used to synthesize **7**. Reactants **1** (0.50 g, 1.4 mmol) and 1,1-diphenylacetone (0.2 g, 2.8 mmol) were used and the reaction was carried out at room temperature for 1 h. A pale-orange solid was obtained that was recrystallized from a dichloromethane/pentane mixed solution at –20 °C to yield 0.686 g of the final product (yield 63.0%). ^{1}H NMR (CDCl$_3$): δ = 0.85 (s, 18 H, NCMe$_3$), 1.26 (d, J_{HH} = 5.1 Hz, 6 H, C*H*$_3$CHO), 2.42 (s, 3 H, toluene CH$_3$), 3.66, 4.21 (dd, $^2J_{HH}$ = 16.8 Hz, 4 H, C*H*$_2$NCMe$_3$), 3.85 (d, J_{HH} = 8.1 Hz, 2 H, Ph$_2$C*H*), 4.90 (m, J_{HH} = 6.3 Hz, 2 H, CH$_3$C*H*O), 5.92 (s, 2 H, pyrrolyl CH), 6.44 (s, 2 H, pyrrolyl CH), 6.71 (s, 2 H, pyrrolyl CH), 7.19–7.51 (m, phenyl CH, toluene CH) ppm. ^{13}C{^{1}H} NMR (CDCl$_3$): δ = 21.4 (q, J_{CH} = 26 Hz, toluene CH$_3$), 25.3 (q, J_{CH} = 126 Hz, *C*H$_3$CHO), 28.4 (q, J_{CH} = 125 Hz, NC*Me*$_3$), 43.3 (t, J_{CH} = 141 Hz, *C*H$_2$NCMe$_3$), 56.2 (s, N*C*Me$_3$), 62.5 (d, J_{CH} = 126 Hz, CH$_3$*C*HO), 71.1 (d, J_{CH} = 142 Hz, Ph$_2$*CH*), 103.1 (d, J_{CH} = 167 Hz, pyrrolyl CH), 113.7 (d, J_{CH} = 170 Hz, pyrrolyl CH), 120.1 (d, J_{CH} = 181 Hz, pyrrolyl CH), 125.3, 126.1, 128.1, 128.2, 128.3, 128.4, 128.8, 129.0, 137.4, 143.5 (m, phenyl CH, C$_{ipso}$, toluene CH, pyrrolyl C$_{ipso}$) ppm.

[{C$_4$H$_3$N(2-CH$_2$N*t*Bu)}Al{κ*O*,κ*O*-(OCMeCHCOMe)}]$_2$ (8): Similar procedures as for compound **2** were used to synthesize **8**. Reactants **1** (0.50 g, 1.4 mmol) and 2,4-pentanedione (0.28 g, 2.8 mmol) were used and the reaction was carried out at room temperature for 1 h. A yellow powder was obtained that was recrystallized from a dichloromethane/toluene mixed solution at –20 °C to yield 0.55 g of the final product (yield 70.9%). ^{1}H NMR ([D$_8$]toluene, 270 K): δ = 1.06, 1.26, 1.49 (s, 18 H, NCMe$_3$), 1.55 (s, 6 H, OCMe), 1.69 (s, 6 H, OCMe), 4.11 (s, 4 H, C*H*$_2$NCMe$_3$), 5.09 (s, 2 H, OCCHCO), 6.18 (s, 2 H, pyrrolyl CH), 6.70 (s, 2 H, pyrrolyl CH), 6.98 (s, 2 H, pyrrolyl CH) ppm. ^{13}C{^{1}H} NMR ([D$_8$]toluene, 270 K): δ = 26.1 (q, J_{CH} = 128 Hz, OC*Me*), 27.1 (q, J_{CH} = 128 Hz, OC*Me*), 29.7 (q, J_{CH} = 126 Hz, NC*Me*$_3$), 44.6 (t, J_{CH} = 131 Hz, *C*H$_2$NCMe$_3$), 58.4 (s, N*C*Me$_3$), 102.2 (d, J_{CH} = 157 Hz, pyrrolyl CH), 104.3 (d, J_{CH} = 164 Hz, OC*C*HCO), 112.8 (d, J_{CH} = 158 Hz, pyrrolyl CH), 124.0 (d, J_{CH} = 178 Hz, pyrrolyl CH), 140.5 (s, pyrrolyl C$_{ipso}$), 191.6 (s, O*C*CHCO), 197.0 (s, O*C*CHCO) ppm.

[{C$_4$H$_3$N(2-CH$_2$N*t*Bu)}Al{κ*O*,κ*O*-(OCPhCHCOPh)}]$_2$ (9): Similar procedures as for compound **2** were used to synthesize **9**. Reactants **1** (0.50 g, 1.4 mmol) and dibenzoylmethane (0.63 g, 2.8 mmol) were used and the reaction was carried out at room temperature for 1 h. An orange powder was obtained that was recrystallized from a dichloromethane/pentane mixed solution at –20 °C to yield 0.77 g of the final product (yield 68.5%). ^{1}H NMR (CDCl$_3$): δ = 1.27 (br., 18 H, NCMe$_3$), 4.28 (s, 2 H, C*H*$_2$NCMe$_3$), 4.25, 4.69 (dd, $^2J_{HH}$ = 17.1 Hz, 2 H, C*H*$_2$NCMe$_3$), 5.80 (s, 2 H, pyrrolyl CH), 6.12 (t, J_{HH} = 2.7 Hz, 1 H, pyrrolyl CH), 6.27 (t, J_{HH} = 2.7 Hz, 1 H, pyrrolyl CH), 6.35 (s, 1 H, pyrrolyl CH), 6.74 (s, 1 H, pyrrolyl CH), 7.03 (s, 1 H, COCHOC), 7.18 (s, 1 H, COCHOC), 7.40–8.27 (m, 20 H, phenyl CH) ppm. ^{13}C{^{1}H} NMR (CDCl$_3$): δ = 30.1 (q, J_{CH} = 126 Hz, NC*Me*$_3$), 43.7 (t, J_{CH} = 135 Hz, *C*H$_2$NCMe$_3$), 44.5 (t, J_{CH} = 135 Hz, *C*H$_2$NCMe$_3$), 57.8 (s, N*C*Me$_3$), 97.5 (d, J_{CH} = 162 Hz, CO*C*HOC), 98.0 (d, J_{CH} = 163 Hz, CO*C*HOC), 100.6 (d, J_{CH} = 165 Hz, pyrrolyl CH), 100.8 (d, J_{CH} = 165 Hz, pyrrolyl CH), 110.3 (d, J_{CH} = 168 Hz, pyrrolyl CH), 111.0 (d, J_{CH} = 156 Hz, pyrrolyl CH), 122.1 (d, J_{CH} = 179 Hz, pyrrolyl CH), 122.5 (d, J_{CH} = 180 Hz, pyrrolyl CH), 128.1 (d, J_{CH} = 160 Hz, phenyl CH), 128.5 (d, J_{CH} = 161 Hz, phenyl CH), 129.0 (d, J_{CH} = 166 Hz, phenyl CH), 132.3 (d, J_{CH} = 161 Hz, phenyl CH), 133.8 (d, J_{CH} = 162 Hz, phenyl CH), 135.8, 137.5 (s, phenyl C$_{ipso}$), 140.4, 140.9 (s, pyrrolyl C$_{ipso}$), 184.3, 186.9 (s, *C*OCHO*C*) ppm.

[{C$_4$H$_3$N(2-CH$_2$NH*t*Bu)}Al{κ*O*,κ*O*-(PhOC=COPh)}]$_2$ (10): Similar procedures as for compound **2** were used to synthesize **10**. Reactants **1** (0.50 g, 1.4 mmol) and benzil (0.59 g, 2.8 mmol) were used and the reaction was carried out at room temperature for 1 h. A brown solid was obtained that was recrystallized from a dichloromethane/pentane mixed solution at –20 °C to yield 0.73 g of the final product (yield 67.0%). ^{1}H NMR (CDCl$_3$): δ = 1.22 (s, 18 H, NCMe$_3$), 2.32 (t, J_{HH} = 8.4 Hz, 2 H, CH$_2$N*H*CMe$_3$), 3.45, 3.78 (m, 4 H, C*H*$_2$NHCMe$_3$), 5.92 (s, 2 H, pyrrolyl CH), 6.27 (t, J_{HH} = 2.1 Hz, 2 H, pyrrolyl CH), 6.97 (s, 12 H, phenyl CH), 7.07 (s, 2 H, pyrrolyl CH), 7.36 (s, 8 H, phenyl CH) ppm. ^{13}C{^{1}H} NMR (CDCl$_3$): δ = 27.4 (q, J_{CH} = 128 Hz, NC*Me*$_3$), 41.9 (t, J_{CH} = 140 Hz, *C*H$_2$NH*t*Bu), 55.3 (s, N*C*Me$_3$), 103.2 (d, J_{CH} = 167 Hz, pyrrole CH), 111.2 (d, J_{CH} = 161 Hz, pyrrole CH), 122.9 (d, J_{CH} = 181 Hz, pyrrole CH), 126.0, 127.2, 128.8, 129.4 (d, J_{CH} = 170 Hz, phenyl CH), 129.4, 131.6 (s, phenyl C_{ipso}), 133.4, 135.6 (s, Ph*C*OO*C*Ph), 142.5 (s, pyrrole C_{ipso}) ppm.

Crystallographic Structural Determination of 2 and 4–9: All the crystals were mounted in capillaries, transferred to a goniostat, and cooled in a stream of nitrogen at 150 K . Data were collected with a Bruker SMART CCD diffractometer using graphite-monochromated Mo-K_α radiation. Data were corrected for absorption empirically by means of ψ scans. All non-hydrogen atoms were refined with anisotropic displacement parameters. For all structures, the positions of the hydrogen atoms were calculated and constrained in idealized geometries by using a riding model in which the H atom displacement parameters were calculated from the equivalent isotropic displacement parameters of the bound atoms. The structures of compounds were determined by direct methods using SHELXS[22a] and refined by full-matrix least-squares methods on F^2 by using SHELXL.[22b] All the relevant crystallographic data and structure refinement parameters for **2** and **4**–**9** are summarized in Table 1.

CCDC-787609 (for **2**), -787613 (for **4**), -787611 (for **5**), -787610 (for **6**), -787608 (for **7**), -787614 (for **8**), and -787612 (for **9**) contain the supplementary crystallographic data for this paper. These data can be obtained free of charge from The Cambridge Crystallographic Data Centre via www.ccdc.cam.ac.uk/data_request/cif.

Polymerization: All the polymerization reactions were carried out in CH_2Cl_2 in a nitrogen-filled Schlenk line. In a typical reaction, the initiator was first dissolved in the solvent (5 mL) and caprolactone ([M]/[I] = 100) was added. The mixture was then stirred at the selected temperature for a period of time to produce a gel- or solid-like polymer. The process quenched by the gradual addition of acidified water (3% CH_3COOH). The resulting solid was washed with hexane and dried to give a satisfactory yield.

The molecular weights of the polymers were determined by gel permeation chromatography (GPC) using a Waters RI 2414 instrument and 1515 pump. M_n and M_w values were determined from calibration plots established with polystyrene standards.

Supporting Information (see footnote on the first page of this article): ^1H–^{13}C HSQC 2D NMR spectra of the compounds.

Acknowledgments

The authors gratefully acknowledge the National Science Council of Taiwan for financial assistance. J. H. H. would also like to thank the National Changhua University of Education for providing the X-ray facility.

[1] a) M. Ephritihine, *Chem. Rev.* **1997**, *97*, 2193; b) R. G. Pearson, *Chem. Rev.* **1985**, 41; c) T. Bauer, S. Schulz, H. Hupfer, M. Nieger, *Organometallics* **2002**, *21*, 2931; d) A. R. Kunicki, A. Chojecki, J. Zachara, M. J. Gliński, *Organomet. Chem.* **2002**, *31*, 136; e) Y. Peng, G. Bai, H. Fan, D. Vidovic, H. W. Roesky, J. Magull, *Inorg. Chem.* **2004**, *43*, 1217; f) K. Igawa, K. Tomooka, *Angew. Chem.* **2006**, *118*, 238; *Angew. Chem. Int. Ed.* **2006**, *45*, 232.

[2] a) M. L. H. Green, D. J. Jones, *Adv. Inorg. Chem. Radiochem.* **1965**, *7*, 115; b) J. P. McCue, *Coord. Chem. Rev.* **1973**, *10*, 265; c) A. P. Humphries, H. D. Kaesz, *Prog. Inorg. Chem.* **1979**, *25*, 145; d) A. P. Borisov, V. D. Makhaev, K. N. Semenenko, *Koord. Khim.* **1980**, *6*, 1139; e) R. G. Teller, R. Bau, *Struct. Bonding (Berlin)* **1981**, *44*, 1; f) R. H. Crabtree in *Encylopedia of Inorganic Chemistry* (Ed.: R. B. King), Wiley, Chichester, **1994**, vol. 3, p. 1392; g) R. Bau, M. H. Drabnis, *Inorg. Chim. Acta* **1997**, *259*, 27.

[3] a) S. Matsui, M. Mitani, J. Saito, Y. Tohi, H. Makio, H. Tanaka, T. Fujita, *Chem. Lett.* **1999**, 1263; b) S. Matsui, Y. Tohi, M. Mitani, J. Saito, H. Makio, H. Tanaka, M. Nitabaru, T. Nakano, T. Fujita, *Chem. Lett.* **1999**, 1065; c) S. Kojoh, T. Matsugi, J. Saito, M. Mitani, T. Fujita, N. Kashiwa, *Chem. Lett.* **2001**, 822.

[4] a) J. Tian, G. W. Coates, *Angew. Chem.* **2000**, *112*, 3772; *Angew. Chem. Int. Ed.* **2000**, *39*, 3626; b) J. Tian, P. D. Hustad, G. W. Coates, *J. Am. Chem. Soc.* **2001**, *123*, 5134.

[5] a) V. C. Gibson, S. Mastroianni, C. Newton, C. Redshaw, G. A. Solan, A. J. P. White, D. J. Williams, *J. Chem. Soc., Dalton Trans.* **2000**, 1969; b) D. J. Jones, V. C. Gibson, S. Green, P. J. Maddox, *Chem. Commun.* **2002**, 1927.

[6] a) C. Wang, S. Friedrich, T. R. Younkin, R. T. Li, R. H. Grubbs, D. A. Bansleben, M. W. Day, *Organometallics* **1998**, *17*, 3149; b) T. R. Younkin, E. F. Connor, J. I. Henderson, S. K. Friedrich, R. H. Grubbs, D. A. Babsleben, *Science* **2000**, *287*, 460.

[7] a) B. L. Small, M. Brookhart, A. M. A. Bennett, *J. Am. Chem. Soc.* **1998**, *120*, 4049; b) G. J. P. Britovsek, V. C. Gibson, B. S. Kimberley, P. J. Maddox, S. J. McTavish, G. A. Solan, A. J. P. White, D. J. Williams, *Chem. Commun.* **1998**, 849; c) B. L. Small, M. Brookhart, *J. Am. Chem. Soc.* **1998**, *120*, 7143; d) G. J. P. Britovsek, S. Mareoinni, G. A. Solan, S. P. D. Baugh, C. Redshaw, V. C. Gibson, A. J. P. White, D. J. Williams, M. R. J. Elsegood, *Chem. Eur. J.* **2000**, *6*, 2221.

[8] R. Kempe, *Angew. Chem.* **2000**, *112*, 478; *Angew. Chem. Int. Ed.* **2000**, *39*, 468.

[9] L. H. Gade, *Chem. Commun.* **2000**, 173.

[10] a) Z. Yu, J. M. Wittbrodt, A. Xia, M. J. Heeg, H. B. Schlegel, C. H. Winter, *Organometallics* **2001**, *20*, 4301; b) P. T. Lansbury, J. R. Rogozinski, F. L. Coblentz, *J. Org. Chem.* **1961**, *26*, 2277.

[11] C.-Y. Lin, C.-F. Tsai, H.-J. Chen, C.-H. Hung, R.-C. Yu, P.-C. Kuo, H. M. Lee, J.-H. Huang, *Chem. Eur. J.* **2006**, *12*, 3067.

[12] a) P.-C. Kuo, I.-C. Chen, J.-C. Chang, M.-T. Lee, C.-H. Hu, C.-H. Hung, H. M. Lee, J.-H. Huang, *Eur. J. Inorg. Chem.* **2004**, 4898; b) J.-C. Chang, C.-H. Hung, J.-H. Huang, *Organometallics* **2001**, *20*, 4445; c) C.-Y. Lin, H. M. Lee, J.-H. Huang, *J. Organomet. Chem.* **2007**, *692*, 3718.

[13] Y.-C. Chen, C.-Y. Lin, C.-Y. Li, J.-H. Huang, L.-C. Chang, T.-Y. Lee, *Chem. Eur. J.* **2008**, *14*, 9747.

[14] a) A. J. R. Son, M. G. Thorn, P. E. Fanwick, I. P. Rothwell, *Organometallics* **2003**, *22*, 2318; b) C. Stanciu, A. F. Richards, M. Stender, M. M. Olmstead, P. P. Power, *Polyhedron* **2006**, *25*, 477; c) D. A. Dickie, I. S. MacIntosh, D. D. Ino, Q. He, O. A. Labeodan, M. C. Jennings, G. Schatte, C. J. Walsby, J. A. C. Clyburne, *Can. J. Chem.* **2008**, *86*, 20.

[15] C. S. Weinert, A. E. Fenwisk, P. E. Fenwick, I. P. Rothwell, *Dalton Trans.* **2003**, 532.

[16] a) O. M. Kekia, L. K. Krannich, C. L. Watkins, C. D. Incarvito, A. L. Rheingold, *Organometallics* **2002**, *21*, 5987; b) E. K. Styron, C. H. Lake, C. H. Watkins, L. K. Krannich, *Organometallics* **1998**, *17*, 4319; c) O. M. Kekia, C. L. Watkins, L. K. Krannich, A. L. Rheingold, L. M. Liable-Sands, *Organometallics* **2001**, *20*, 582; d) D. S. Brown, A. Decken, C. A. Schnee, A. H. Cowley, *Inorg. Chem.* **1995**, *34*, 6415.

[17] A. D. Becke, *J. Chem. Phys.* **1993**, *98*, 5648.

[18] C. Lee, W. Yang, R. G. Parr, *Phys. Rev. B* **1988**, *37*, 785.

[19] M. J. Frisch, G. W. Trucks, H. B. Schlegel, G. E. Scuseria, M. A. Robb, J. R. Cheeseman, J. A. Montgomery Jr., T. Vreven, K. N. Kudin, J. C. Burant, J. M. Millam, S. S. Lyengar, J. Tomasi, V. Barone, B. Mennucci, M. Cossi, G. Scalmani, N. Rega, G. A. Petersson, H. Nakatsuji, M. Hada, M. Ehara, K. Toyota, R. Fukuda, J. Hasegawa, M. Ishida, T. Nakajima, Y. Honda, O. Kitao, H. Nakai, M. Klene, X. Li, J. E. Knox, H. P. Hratchian, J. B. Cross, C. Adamo, J. Jaramillo, R. Gomperts,

R. E. Stratmann, O. Yazyev, A. J. Austin, R. Cammi, C. Pomelli, J. Ochterski, P. Y. Ayala, K. Morokuma, G. A. Voth, P. Salvador, J. J. Dannenberg, V. G. Zakrzewski, S. Dapprich, A. D. Daniels, M. C. Strain, O. Farkas, D. K. Malick, A. D. Rabuck, K. Raghavachari, J. B. Foresman, J. V. Ortiz, Q. Cui, A. G. Baboul, S. Clifford, J. Cioslowski, B. B. Stefanov, G. Liu, A. Liashenko, P. Piskorz, I. Komaromi, R. L. Martin, D. J. Fox, T. Keith, M. A. Al-Laham, C. Y. Peng, A. Nanayakkara, M. Challacombe, P. M. W. Gill, B. Johnson, W. Chen, M. W. Wong, C. Gonzalez, J. A. Pople, *Gaussian 03*, rev. B.05, Gaussian, Inc., Pittsburgh, PA, **2003**.

[20] P. Dubois, I. Barakat, R. Jerome, P. Teyssie, *Macromolecules* **1993**, *26*, 4407.

[21] C.-T. Chen, C.-A. Huang, B.-H. Huang, *Macromolecules* **2004**, *37*, 7968.

[22] a) G. M. Sheldrick, *SHELX97, Programs for Crystal Structure Analysis: Structure Determination (SHELXS)*, University of Göttingen, Germany, **1997**; b) G. M. Sheldrick, *SHELX97, Programs for Crystal Structure Analysis: Refinement (SHELXL)*, University of Göttingen, Germany, **1997**.

Received: January 11, 2011